On Lithium Wall and Performance of Magnetic Fusion Device

S. I. Krasheninnikov[1] , L. E. Zakharov[2], and G. V. Pereverzev[3]

[1]University California San Diego, La Jolla, USA

[2]Princeton Plasma Physics Laboratory, Princeton, USA

[3]Max-Planck-Institut für Plasmaphysik, Garching bei München, Germany

Abstract

It is shown that lithium walls resulting in zero recycling conditions at the edge of magnetic fusion device can cause drastic reduction of heat conduction energy loss from the core and, therefore, can crucially alter the performance of magnetic fusion device.

During recent years the idea of potentially very strong impact of fully absorbing lithium walls on the performance of magnetic fusion devices have been reported by the authors many times on different meetings. However, finding again and again the necessity to explain why lithium wall can crucially alter the performance of magnetic fusion devices we decided to publish the essence of our presentations on this particular topic along with some preliminary modeling of the impact of lithium walls on next step device performance in this brief communication. The paper devoted to a much broader scope of the issues of applications of lithium to magnetic fusion will be published elsewhere.

What makes lithium to be so special material for the first wall of magnetic fusion devices is practically complete absorption of impinging protons (and other hydrogen isotopes) which is associated with the formation of lithium hydride. This feature results in zero recycling of the plasma on lithium surface when practically there is no hydrogen comes back from the surface into the plasma. (We assume that lithium is not saturated with hydrogen.) We will show that zero recycling conditions causes drastic reduction of heat conduction energy loss from the core and by that can crucially alter the performance of magnetic fusion devices. As an example we will consider a tokamak, but the conclusions of our analysis can be applied to all magnetic fusion devices.

The simplest form of the plasma energy transport equation in a tokamak can be written as follows

$$Q_\Gamma(\rho) + Q_{\nabla T}(\rho) \equiv 5\,T\,\Gamma_p(\rho) - K(\rho)\frac{dT}{d\rho} = Q_p(\rho), \qquad (1)$$

where T is the plasma temperature (for simplicity we assume here $T_e = T_i$), ρ is the effective coordinate going from the center of the machine all the way to the wall ($0 \le \rho \le 1$), $\Gamma_p(\rho)$ and $Q_p(\rho)$ are the plasma particle and energy flux, $K(\rho)$ is the effective heat conduction coefficient. The first term on the left hand side of Eq. (1) describes convective part of the energy flux while the second one is the simplest account for conduction part.

To close the equation (1) we need to use the relation between plasma energy, $Q_p^w = Q_p(\rho = 1)$, and particle, $\Gamma_p^w = \Gamma_p(\rho = 1)$, flux to neutralizing material wall at tokamak edge ($\rho = 1$). For the case where the distribution function of plasma particles coming to the wall is described

by only one parameter (e. g. effective temperature) we have (see for example Ref. 1 where the coupling of the edge and core plasmas is discussed in details)

$$T_w = \frac{Q_p^w}{\gamma\,\Gamma_p^w}, \qquad (2)$$

where $\gamma = \gamma_e + \gamma_i \sim 6 \div 8$ and $\gamma_e \sim \gamma_i \sim 3 \div 4$ are so-called energy transmission coefficient, T_w is the averaged plasma temperature near the wall, $T_w = T(\rho = 1)$.

From the Eqs. (1) and (2) we find the contributions of conductive ($Q_\Gamma^w = Q_\Gamma(\rho = 1)$) and conductive ($Q_{\nabla T}^w = Q_{\nabla T}(\rho = 1)$) parts of the energy flux at the edge are

$$\frac{Q_\Gamma^w}{Q_p^w} = \frac{5}{\gamma}, \qquad (3a)$$

$$\frac{Q_{\nabla T}^w}{Q_p^w} = \frac{\gamma - 5}{\gamma}. \qquad (3b)$$

As we see from Eq. (3), at the vicinity of the wall most of the energy flux is carried by convection. For known profiles of $\Gamma_p(\rho)$ and $Q_p(\rho)$ we can solve the equations (1), (2). Qualitative solution of Eqs. (1), (2) is shown in Fig. 1 for constant $Q_p(\rho)$ and the plasma source localized at $\rho \approx \rho_\Gamma$. As one sees from Fig. 1, there are two distinctive regions of the temperature variation. In one of the regions, $\rho < \rho_\Gamma$, the energy is transported by conduction causing a strong temperature gradient. In another one, $\rho_\Gamma < \rho \le 1$, significant part of the energy is transported by convection which results in rather flat temperature profile: $T_\Gamma < (\gamma/5)T_w$.

In conventional tokamaks flux Γ_p^w is determined mainly by recycling processes including the plasma surface neutralization and volumetric recombination with the following ionization of originated neutrals. The contributions of both gas puffing and pumping are small

$$\left(\Gamma_p^w\right)_{conventional} >> \Gamma_{puf},\quad \Gamma_{pump}, \qquad (4)$$

where Γ_{puf} (Γ_{pump}) is the puffing (pumping) particle flux (by puffing we assume here all sorts of hydrogen injection into tokamak). Therefore, the magnitude of plasma flux Γ_p^w is governed by such hardly controlled recycling processes as plasma cross-field transport; reflection, absorption, and desorption of hydrogen at the wall; and the transport of neutral hydrogen back to the plasma including neutral-plasma interactions and hydrogen ionization process. Moreover, due to relatively large plasma transport in the recycling region at the edge, the flux Γ_p^w appears to be very large and, therefore, the temperature T_w is, correspondingly, small ($T_w \sim 10-100$ eV) in comparison with central temperature. As a result, large temperature gradient drives ion temperature gradient (ITG) instability resulting in large conductive energy losses and poor plasma performance (e. g. see Ref. 2).

However, the situation can be radically changed if the wall completely absorbs incoming plasma flux like lithium wall does. In this case

$$\left(\Gamma_p^w\right)_{\text{Li wall}} = \Gamma_{puf} = \Gamma_{absorb}. \tag{5}$$

Moreover, both magnitude and location of plasma source can be controlled by hydrogen injection. Then with a proper choice of the location of hydrogen injection, for the same plasma density and energy flux, the magnitude of Γ_p^w can be much smaller and T_w, correspondingly, much higher then in conventional tokamak (see Fig. 2). As a result, temperature gradient in the core can be reduced below the level critical for ITG instability causing drastic improvement of plasma confinement.

As an example of the impact of fully absorbing lithium wall and zero recycling conditions on a tokamak performance we present here some results of the modeling of the performance of the ITER-FEAT [3] assuming fully absorbing boundary. For the modeling we use transport code ASTRA [4]. For the heat, $\chi_{e/i}$, and particle, D, diffusivities we use

$$\chi_e = \chi_e^{neo} + \chi_e^{ITG} + \min\left\{\chi_{Bohm}, \chi_e^{T-11}\right\}, \tag{6a}$$

$$\chi_i = \chi_i^{neo} + \chi_i^{ITG}, \tag{6b}$$

$$D = D^{neo} + 0.1 \times \left\{ \left(\chi_i - \chi_i^{neo} \right) + \left(\chi_e - \chi_e^{neo} \right) \right\}, \qquad (6c)$$

where χ_e^{neo}, χ_i^{neo}, and D^{neo} are the neoclassical heat and particle diffusivities, χ_e^{ITG} and χ_i^{ITG} are electron and ion heat diffusivities associated with the ITG instability taken from [2], χ_{Bohm} is the Bohm diffusion coefficient, and χ_e^{T-11} is the Ohkawa type scaling from [5]. Neoclassical particle pinch is also accounted for in the plasma density transport equation. We assume 30 MW of the neutral beam and 10 MW of the ICRF auxiliary heating. We also adopt 5% dilution of the plasma due to helium and ???5% due to beryllium.

As the boundary conditions for the plasma density and both electron and ion temperatures at the wall we used the model from Ref. 1 which, in particular, relates the energy fluxes and temperatures in electron and ion components similar to that of Eq. (2). For the modeling presented here we choose $\gamma_e = \gamma_i = 3$.

We apply bell shaped plasma particle source at $\rho = 0.75$ with the magnitude varying to sustain constant volume averaged plasma density of $10^{20}\,m^{-3}$. To model fully absorbing lithium wall we assume no any other plasma particle source. We start with nominal IETR-FEAT regime [3] and find that fusion power runs away. Time history of ion temperature in the center ($T_i(\rho = 0, t)$) and at the wall ($T_i(\rho = 1, t)$), fusion power ($P_{fus}(t)$), and plasma flux to the wall ($\Gamma_w^p(t)$) are shown in Fig. 3. At these times β_N does not exceed 2.5. As one sees from Fig. 3, in accordance with Eq. (2) edge plasma temperatures naturally increase with increasing fusion power. As a result, temperature gradient in the core does not increase with increasing fusion power which allows to avoid a fatal impact of the ITG instability. This is in a sharp contrast to conventional ITER where separatrix plasma temperature is negligibly small and the ITG instability limits the temperature gradient so that the performance of the machine is completely determined by the height of H-mode pedestal.

The plasma density and electron and ion temperature profiles for t=1 sec are shown in Fig. 4. Notice that high edge plasma temperatures significantly increase fusion power yield so that the ITER runs away with averaged energy confinement time ~ 2 s.

In sum, we show that lithium walls resulting in zero recycling conditions at the edge of magnetic fusion device can cause drastic reduction of heat conduction energy loss from the core and, therefore, can crucially alter the performance of magnetic fusion device. As an example we model the ITER-FEAT performance with lithium walls and show that fusion power runs away due to natural increase edge plasma temperature with increasing fusion power which eliminate strong core plasma gradient causing the ITG instability.

Acknowledgments

This research was supported by United States Department of Energy.

References

[1] S. I. Krasheninnikov, P. N. Yushmanov, Sov. J. Plasma Phys., **16** (1990) 801; A. Yu. Dnestrovskij, S. I. Krasheninnikov, P. N. Yushmanov , Nucl. Fusion, **31** (1991) 647.

[2] M. Kotschenreuther, W. Dorland, M. A. Beer, and G. W. Hammet, Phys. Plasmas **2** (1995) 2381.

[3] Y. Shimomura, R. Aymar, V. Chuyanov, M. Huget, H. Matsumoto, T. Mizoguchi, Y. Murakami, A. Polevoi, M. Shimada and the ITER Joint Central Team and Home Teams, "ITER-FEAT Operation" 18th IAEA Fusion Energy Conference, Sorrento, Italy, 4-10 October 2000, Paper ITER/1.

[4] G. Pereverzev and P. N. Yushmanov, "ASTRA Automated System for Transport Analysis in a Tokamak", Max-Planck-Institut fur Plasmaphysik, IPP 5/98, February 2002.

[5] A. G. Barsukov et al., 9th IAEA Conference on Plasma Physics and Controlled Nuclear Fusion Research, Baltimore, 1982 (IAEA, Vienna, V. 1 (1983) 83).

Figure Captions

Fig. 1. Qualitative dependence $T(\rho)$ of the solution of Eqs. (1), (2).

Fig. 2. Schematic dependence of $T(\rho)$ for both conventional and lithium wall tokamaks.

Fig. 3. Time history of ion central, $T_i(\rho = 0, t)$, and wall, $T_i(\rho = 1, t)$, temperatures, fusion power, $P_{fus}(t)$, and plasma flux to the wall, $\Gamma_w^p(t)$.

Fig. 4. The plasma density, $n_e(\rho)$, electron, $T_e(\rho)$, and ion, $T_i(\rho)$, temperature profiles for t=1 sec. On the top panel the shape of plasma particle source, $S_e(\rho)$, is also shown.

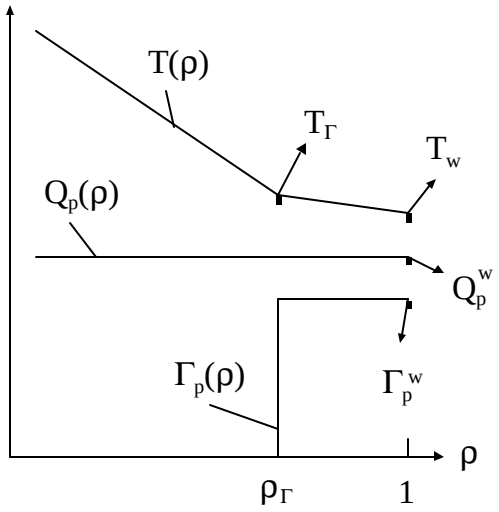

Fig. 1.

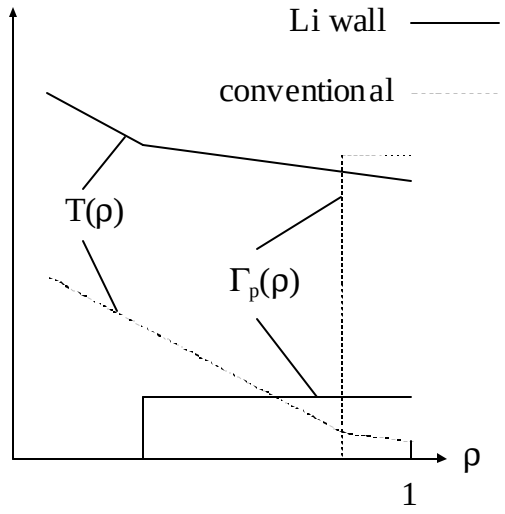

Fig. 2.

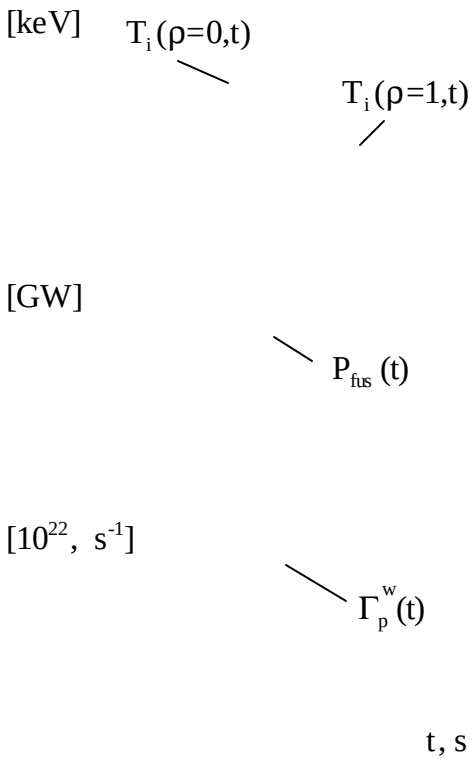

Fig. 3.

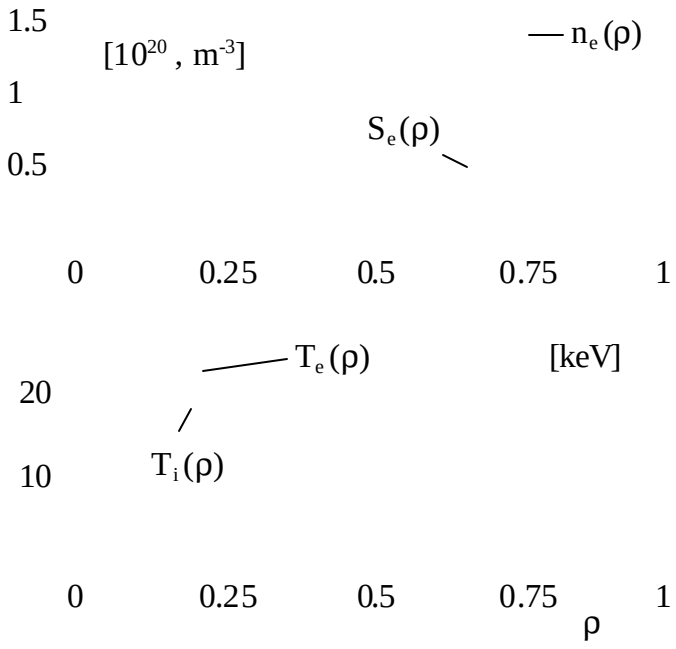
1.5
[10^20 , m^-3]
— n_e (ρ)
1
S_e (ρ)
0.5
0
0.25
0.5
0.75
1
T_e (ρ)
[keV]
20
T_i (ρ)
10
0
0.25
0.5
0.75
1
ρ

Fig. 4.